Mechanical Properties of Ultra-thin Nb_3Sn Composite Wires

M. Sugano, A. Kikuchi, H. Kitaguchi, G. Nishijima and T. Yagai

***Abstract*—Flexible Rutherford cables are needed to realize high field superconducting magnets with A15 conductors based on the react-and-wind (R&W) technology. Aiming such an application, ultra-thin A15 composite wires with a diameter of 0.03–0.05 mm have been developed by the National Institute for Materials Science (NIMS).**

Mechanical properties of such ultra-thin Nb_3Sn wires were evaluated to determine the cabling parameters and mechanical analysis of twisted cables. Tensile tests were performed at room temperature for 0.05 mm-thick Nb_3Sn wires before and after heat treatment for the first time. Basic mechanical parameters such as 0.2% proof strength and fracture strength were evaluated from a stress–strain curve. Young's modulus of such a thin wire was determined from unlading and reloading slopes of a load–stroke curve for the specimens with different gauge lengths. Fracture strain was estimated without using extensometers and strain gauges by correcting for machine deformation. Based on these results, we concluded that a simple technique to measure stress–strain curves for ultra-thin Nb_3Sn wires was able to be established.

***Index Terms*—Ultra-thin Nb_3Sn wire, single fiber tensile test, Fracture strength, Young's modulus**

I. Introduction

NB3SN is one of the promising candidate materials for high field accelerator magnets [1]. However, the mechanical weakness of Nb_3Sn has made magnet development more challenging. Since Nb_3Sn is an intermetallic compound, its fracture strain is less than 0.4% in the state-of-the-art conductors used for accelerator magnets [2]. Moreover, the critical current of Nb_3Sn wires is significantly suppressed even by elastic deformation [3]. Due to such intrinsic strain sensitivity, stress and strain management of Nb_3Sn conductors is of key importance in Nb_3Sn magnets.

To avoid mechanical damage during coil winding, Nb_3Sn coils are generally fabricated by the wind-and-react (W&R) method. However, the W&R method has several drawbacks. The coil parts, insulation material and tooling for coil winding need to have resistance to reaction temperature higher than 650ºC [1]. A special furnace is necessary to react long coils for accelerator magnets [4], which makes coil fabrication more costly. For these reasons, the react-and-wind (R&W) technology is required for Nb_3Sn coils.

In a composite wire, Nb_3Sn filaments are embedded in Cu or Cu alloy matrix. When the wire is bent during coil winding, Nb_3Sn filaments are subjected to axial strain depending on a distance from the neutral axis. In order to reduce such bending strain, ultra-thin A15 type composite wires has been proposed by the National Institute for the Materials Science (NIMS) [5][6]. Nb_3Sn and Nb_3Al strands with a diameter of 0.03–0.05 mm have been successfully fabricated. These values are equivalent to typical Nb_3Sn filament or sub-element diameter in wires with a diameter of 0.8–1 mm [7]. When a twisted cable composed of such thin wires is bent, each strand can slide with each other. Therefore, bending strain proportional to the wire diameter can be significantly reduced. This concept was validated in 7 stranded cables and 7×7 stranded cables [6].

Based on this idea, more flexible Rutherford cable can be expected. Twisted cables will be fabricated with non-reacted wires and then the cables will be reacted before coil winding. To determine the cabling parameters such as wire tension, stress–strain curves of non-reacted wires are necessary. For the mechanical analysis of twisted cables, characteristic parameters of proof strength, fracture stress/strain and Young's modulus of reacted wires are needed. For these purposes, mechanical properties of 0.05 mm-thick Nb_3Sn wires were evaluated by tensile test at the present study.

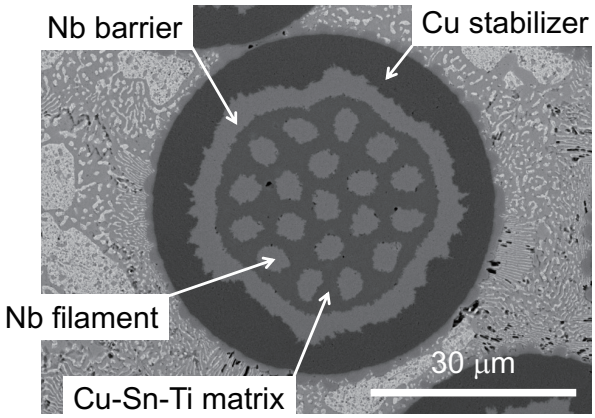

Fig. 1. Cross-sectional image of non-reacted 0.05 mm-thick Nb_3Sn wire.

This work was supported by Grants-in-Aid for Scientific Research A (21H04477).

M. Sugano is with Cryogenics Science Center, High Energy Accelerator Research Organization (KEK), Tsukuba 305-0801, Japan (e-mail: michinaka.sugano@kek.jp).

A. Kikuchi, H. Kitaguchi and G. Nishijima are with the National Institute for Materials Science (NIMS), Tsukuba 305-0003, Japan.

T. Yagai is with Sophia University, Tokyo 102-8554, Japan.

II. Experimental Procedure

A Nb_3Sn wire with a diameter of 0.05 mm (SK217) was provided from NIMS. A cross-section of this wire before heat-treatment is shown in Fig. 1. The wire having 19 Nb filaments was fabricated through the bronze process. Cu-Sn-Ti matrix is surrounded by a Nb barrier. The outer most layer is a stabilizing Cu. Cu/non-Cu ratio is 1. A piece length of this wire longer than 7 km has been achieved, demonstrating good drawability and feasibility of mass production [6]. Maximum temperature and duration of heat-treatment for formation of Nb_3Sn were 665°C and 200 h, respectively. Current density in the non-Cu area (non-Cu J_c) at 4.2 K and 12 T is 426 A/mm^2.

Tensile test was performed at room temperature for the wires before and after heat-treatment. A variety of strain measurement devices for small-sized specimens including a video extensometer [8], optical interferometer [9], and digital image correlation (DIC) [10] have been developed. These non-contact extensometers are useful but costly. In this study, the single-filament method developed in the field of carbon and glass fiber-reinforced composite materials was selected [11]-[13]. This method can be applied to a filament with a diameter of less than 10 μm. On the other hand, one of the drawbacks of this method is that only average strain over the whole gauge length can be measured, which is the same as conventional extensometers [14]. Therefore, the applicable strain region is limited below a few percent. In addition, this method should not be adopted when the machine compliance is comparable to that of a specimen, which is not the case in the present study.

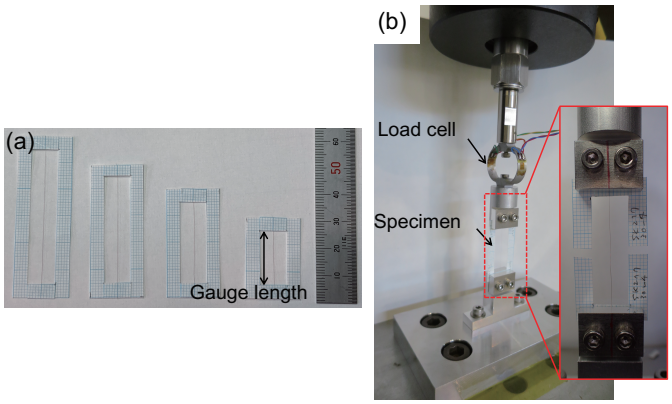

Fig. 2. Specimens with a gauge length of 20–50 mm (a) and setup for single fiber tensile test (b). The inset is a magnified view to show how to grip a specimen.

As shown in Fig. 2(a), a thin wire was put along a line on a grid paper frame, then both ends of the wire were bonded with cyanoacrylate adhesive. The specimens with a gauge length from 20 to 50 mm were prepared. Then the specimen was attached to a commercial tensile testing machine (Shimadzu, AG-5000C). To prevent sample bending due to misalignment of the wire and the tensile axis, the line of the graph paper was aligned with the scratch line drawn on the upper and lower grips before fastening the screws. The setup of tensile test is shown in Fig. 2(b). Before applying tensile load, the side of the paper frame was cut so that the load is only carried by the Nb_3Sn wire.

A dedicated load cell with a load capacity of 5 N was fabricated with a high strength aluminum alloy (A7075) frame and strain gauges. This load cell was calibrated using weights whose accuracy is better than $6x10^{-4}$%. Good linearity was confirmed up to 3 N which is sufficient load for the present test.

Stroke of the tensile testing machine was also inspected using a preliminary calibrated linear gauge. The machine stroke was confirmed to have the accuracy within 0.1%.

Tensile speed was set to be 0.3 mm/min. To evaluate Young's modulus from a load–stroke curve, unloading was performed from the load at 0.5 N and 0.2 N for non-reacted and reacted wires, respectively. Then the test was continued until overall fracture of the specimen occurred.

Fracture surface of the wires after tensile test was observed using a scanning electron microscope (SEM).

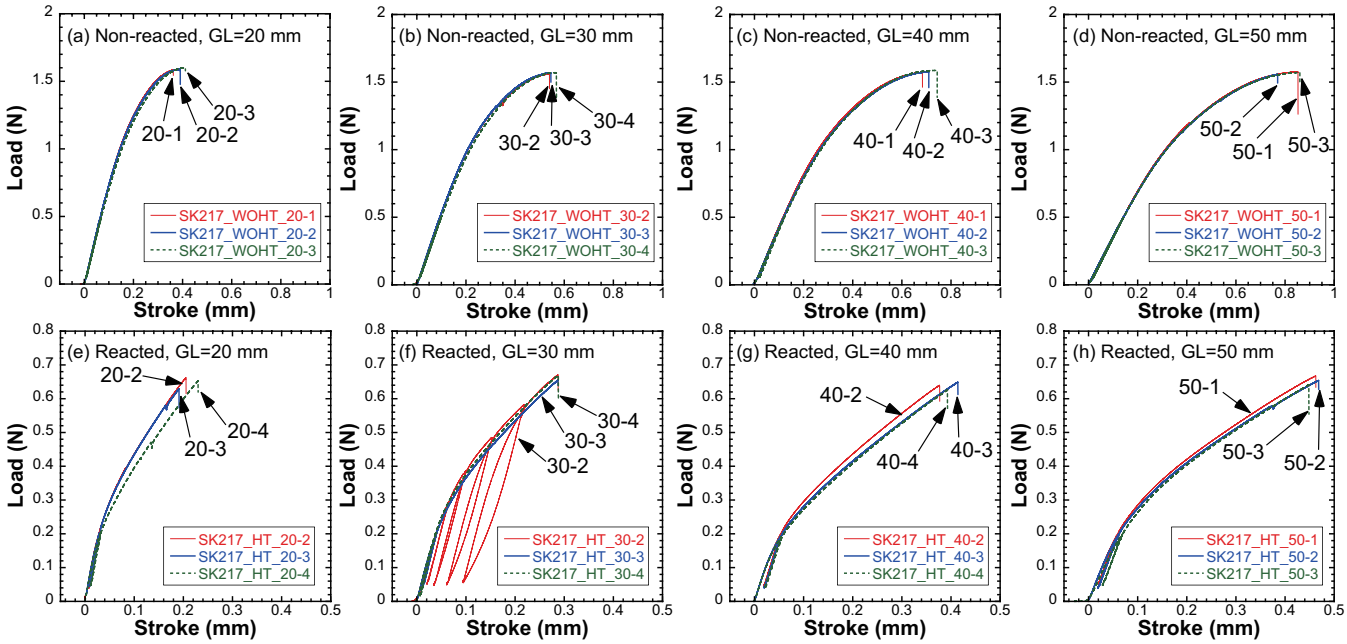

Fig. 3. Load-stroke curves for non-reacted and reacted Nb_3Sn wires with the gauge length (GL) of 20, 30, 40, and 50 mm.

III. Results and Discussion

A. Load–stroke curves

Fig. 3 shows load–stroke curves of the wires before and after heat-treatment. The curves of three specimens for each gauge length agree well with each other. Fracture position of all the specimens of non-reacted wires and 70% of the specimens of reacted wires were within the gauge. There was no dependence in fracture load on the fracture position.

Table I summarizes the measured characteristic mechanical parameters. Fracture strength was evaluated from the fracture load and a cross-sectional area calculated with the nominal wire diameter of 0.05 mm. The wire diameter was also confirmed to be 0.05 mm by the polished cross-sectional image shown in Fig. 1. Average fracture load for non-reacted and reacted wires are 1.58 N and 0.65 N, respectively. These correspond to fracture strength of 803 and 332 MPa, respectively. Within this study, no gauge length dependence in fracture strength was found. The main reason of higher strength in the non-reacted wire is due to work-hardening by drawing. 0.2% proof strength using Young's modulus determined in IIIB was evaluated to be 624 and 205 MPa for non-reacted and reacted wires, respectively.

TABLE I
Measured Characteristic Mechanical Properties of Nb_3Sn Wires Before and After Heat-Treatment.

Before heat-treatment			
Gauge length (mm)	0.2% proof strength (MPa)	Fracture load (N)	Fracture strength (MPa)
20	629±37	1.59±0.01	810±4
30	612±18	1.57±0.01	800±7
40	623±11	1.58±0.01	804±4
50	632±3	1.57±0.01	798±4
Average	624±20	1.59±0.01	803±6
After heat-treatment			
Gauge length (mm)	0.2% proof strength (MPa)	Fracture load (N)	Fracture strength (MPa)
20	199±16	0.65±0.02	330±8
30	223±10	0.67±0.01	339±4
40	185±10	0.65±0.01	331±5
50	213±6	0.65±0.01	333±7
Average	205±18	0.65±0.01	332±7

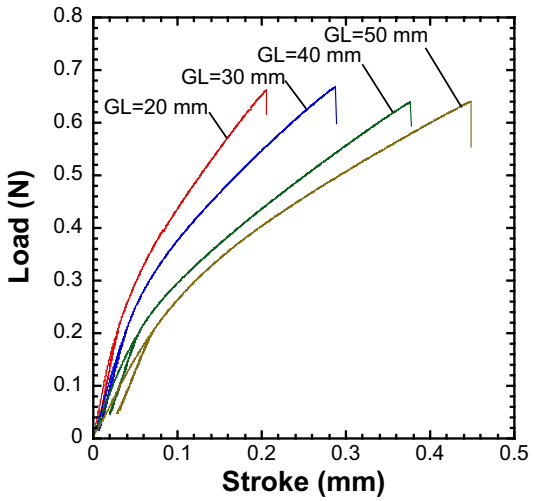

Fig. 4. Load-stroke curves for reacted Nb_3Sn wires with a gauge length (GL) of 20–50 mm.

Fig. 4 shows comparison of load–stroke curves for the specimens with difference gauge lengths. The longer gauge length of a specimen is, the more elongation of the specimen at the same load is.

B. Observation of Fracture Surface

Fig. 5 shows SEM images of fracture surface. More significant necking was confirmed in non-reacted wires as shown in Fig. 5(a) and (c). Knife-edge-type fracture morphology in metal components exhibit ductile fracture in non-reacted wires. In reacted wires, Nb_3Sn filaments and reacted Nb barrier exhibit brittle fracture surface. As can be seen in Fig. 5(d), Kirkendall voids with a diameter of 3.5 μm exist between Nb_3Sn filaments.

C. Evaluation of Young's Modulus

Young's modulus of the wires was evaluated from the unloading and reloading slopes of a load–stroke curve. The stroke includes both elongation of a specimen and deformation of testing machine. As shown in Fig. 4, a longer sample elongates

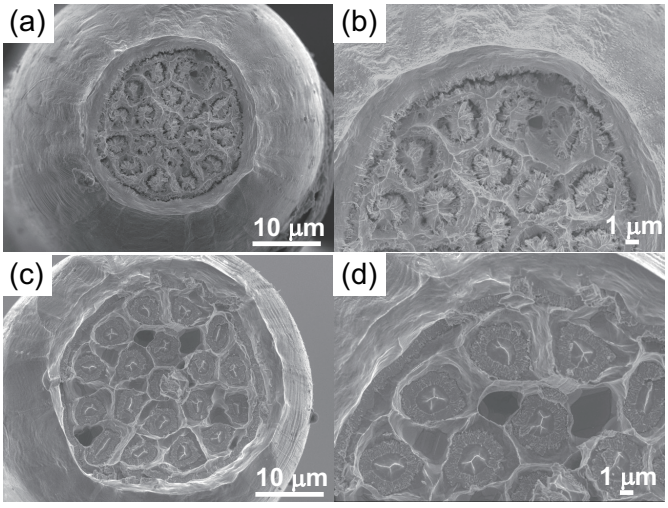

Fig. 5. SEM images of fracture surface for non-reacted ((a) and (b)) and reacted ((c) and (d)) wires.

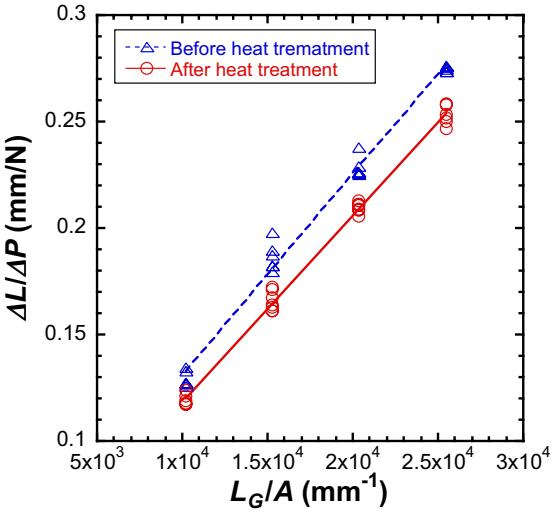

Fig. 6. Plot corresponding to equation 1. From the inverse slope and y-intercept of the linear fit, Young's modulus and compliance can be evaluated.

TABLE II
MEASURED YOUNG'S MODULUS OF NON-REACTED AND REACTED NB3SN WIRES AND MACHINE COMPLIANCE.

	Young's modulus (GPa)	Compliance (mm/N)
Non-reacted wire	106	3.70×10^{-2}
Reacted wire	114	3.12×10^{-2}

TABLE III
VOLUME FRACTION AND YOUNG'S MODULUS OF EACH COMPONENT USED TO CALCULATE YOUNG'S MODULUS OF NON-REACTED WIRES.

	Volume fraction	Young's modulus (GPa)
Nb filament	0.132	103 [16]
Nb barrier	0.111	103 [16]
Bronze	0.256	113 [8]
Cu	0.500	116 [8]

more at the same load. On the other hand, machine deformation is a function of load. The coefficient of machine deformation is called compliance, and has units of mm/N. This value can be obtained by extrapolating the measured total elongation to the gauge length equal to zero. Then Young's modulus of the specimen can be determined excluding an influence of machine deformation. More detailed procedure is found in [12].

The procedure described above can be expressed by the following equation,

$$\Delta L/\Delta P = 1/E\ \ L_G/A + c \qquad (1)$$

where ΔL, ΔP, E, L_G, A and c are total elongation, change of load, Young's modulus of the specimen, gauge length, cross-sectional area of the wire and compliance of the testing machine, respectively.

As a preliminary test, Young's modulus of SUS304 wire with a diameter of 0.1 mm was evaluated along this method. The measured Young's modulus was 197 GPa, which agrees well with the reported value [15].

Fig. 6 shows the plot corresponding to the equation 1 for non-reacted and reacted Nb_3Sn wires. The values along the horizonal axis are determined only by the dimension of specimens, while those in the vertical axis were obtained from the inverse of unloading and reloading slopes of a load–stroke curve. Young's modulus and compliance evaluated from the least square fit with a linear function are shown in Table II. Young's moduli of non-reacted and reacted wires are 106 and 114 GPa, respectively.

The measured Young's modulus of non-reacted wire was compared with the calculated value based on the rule-of-mixture. Table III summarizes parameters used for this calculation. Volume fraction of each component was evaluated by image analysis of the cross-sectional image shown in Fig. 1. Young's moduli of the constituent materials were cited from [8][16]. The Young's modulus for the non-reacted wire from these values was calculated to be 112 GPa, which shows good agreement with the measured value. 6% higher calculated value than the measurement is partially due to Young's modulus of Nb. For the calculation, Young's modulus of 103 GPa for Nb bulk was used [16]. As is well known, however, Nb has drawing texture along the <110> direction [17], which coincides the direction with the lowest elastic modulus of 93 GPa [18]. If this value is adopted, calculated Young's modulus of the non-reacted wire is 110 GPa.

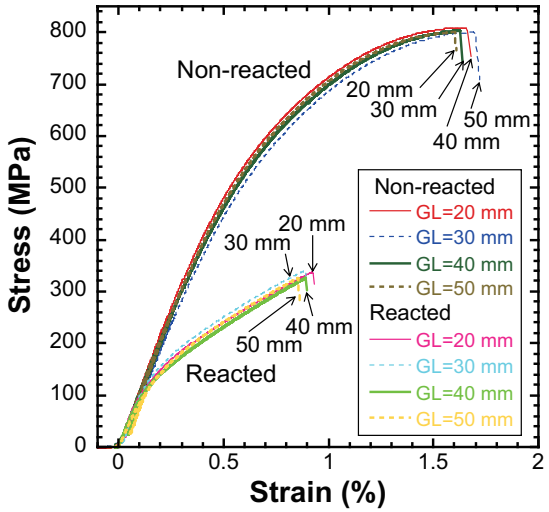

Fig. 7. Stress-strain curves for non-reacted and reacted Nb_3Sn wires after correction of machine deformation.

D. Correction of Machine deformation

Sample strain was calculated by the following equation, considering correction of machine deformation

$$\varepsilon = (\Delta L_s + \Delta L_t - cP)/L_G \times 100 \qquad (2).$$

In this equation, ΔL_s, ΔL_t and P are the elongation of a specimen and a testing machine, and load, respectively. Fig. 7 shows stress-strain curves after correcting for machine deformation. The compliance for non-reacted and reacted wire in Table II were used. As shown in this plot, the stress-strain curves for the specimens with different gauge lengths fall onto the same curve. Average fracture strain was evaluated to be 1.62±0.09% and 0.91±0.05% for non-reacted and reacted wires, respectively. The fraction of machine deformation to the total elongation at sample fracture is 6–19%, which is not negligible. The case with the maximum error corresponds to the non-reacted wire with a gauge length of 20 mm in which fracture load is higher than that of the reacted wire and the gauge length is the shortest. These results demonstrate that this technique is useful to evaluate strain of thin wire sample to which extensometers and strain gauges could not be directly attached.

IV. CONCLUSION

Mechanical properties of 0.05 mm-thick Nb_3Sn composite wires were evaluated using a tensile testing method developed for single-filaments. Fracture strength and Young's modulus of the wires before and after heat-treatment were successfully determined. Fracture strain was able to be obtained even without extensometers and strain gauges by correcting for machine deformation. Based on these results, we concluded that a simple technique for evaluating the basic mechanical properties of such a thin and brittle Nb_3Sn wire could be established.

As a next step, the maximum allowable load without degradation of critical current will be explored.

REFERENCES

[1] D. Schoerling and A.V. Zlobin, Eds, *Nb_3Sn accelerator magnets*. Cham, Switzerland: Springer, 2019.

[2] N. Cheggour, T. C. Stauffer, W. Starch, L.F. Goodrich, and J.D. Splett, "Implications of the strain irreversibility cliff on the fabrication of particle-accelerator magnets made of restacked-rod-process Nb_3Sn wires," *Sci. Rep.*, vol. 9, Apr. 2019, Art. no. 5466.

[3] A. Godeke, F. Hellman, H.H.J ten Kate, and M.G.T Mentink "Fundamental origin of the large impact of strain on superconducting Nb_3Sn," *Supercond. Sci. Technol.*, vol. 31, Sep. 2018, Art. no. 105011.

[4] F. Lackner, N. Bourcey, P. Ferracin, T. Ohnweiler, P. Revilak, F. Savary, and S. Triquet, "Analysis of temperature uniformity during heat treatment of Nb_3Sn coils for the high-luminosity LHC superconducting magnets," *IEEE Trans. Appl. Supercond.*, vol. 26, no. 4, Jun. 2026, Art. no. 4004205.

[5] A. Kikuchi, Y. Iijima, S. Nimori, M. Yamamoto, M. Kawano, M. Kimura, J. Nagamatsu, M. Otsubo, A. Ichinose, and K. Tsuchiya, "Ultra-fine Nb_3Al mono-core wires and cables," *IEEE Trans. Appl. Supercond.*, vol. 31, no. 5, Aug. 2021, Art. no. 6000105.

[6] A. Kikuchi, Y. Iijima, M. Yamamoto, M. Kawano, and M. Otsubo, "The Bronze processed Nb_3Sn ultra-thin superconducting wires," *IEEE Trans. Appl. Supercond.*, vol. 32, no. 4, Jun. 2022, Art. no. 6000104.

[7] A. Ballarino *et al*, "The CERN FCC conductor development program: a worldwide effort for the future generation of high-field magnets," *IEEE Trans. Appl. Supercond.*, vol. 29, no. 5, Aug. 2019, Art. no. 6000709.

[8] M. Hojo, T. Matsuoka, M. Hashimoto, M. Tanaka, M. Sugano, S. Ochiai, and K. Miyashita, "Direct measurement of elastic modulus of Nb_3Sn using extracted filaments from superconducting composite wire and resin impregnation method," *Phys. C*, vol. 445–448, Jul. 2006, pp.814–818.

[9] D.A. LaVan and W.N. Sharpe, "Tensile Testing of Microsamples," *Exp. Mech.*, vol.39, no. 3, Sep. 1999, pp.210-216.

[10] S. Nazari-Onlaghi, A. Sadeghi, and M. Karimpour, "Design and manufacture of a micro-tensile testing machine for *in situ* optical observation and DIC analysis: application to 3D-printed and compression-molded ABS," *J. Micromech. Microeng.*, vo.31, Mar. 2021, Art. no. 045016.

[11] *Carbon Fibre-Determination of the Tensile Properties of Single-Filament Specimens*, ISO 11566:1996, 1996.

[12] M. Sugano, K. Osamura, and M. Hojo, "Mechanical properties of Bi2223 filaments extracted from multifilamentary tape evaluated by the single-fibre tensile test," *Supercond. Sci. Technol.*, vol. 16, Mar. 2003, pp.57096–8.

[13] M. Sugano, A. Ballarino, B. Bartova, R. Bjoerstad, C. Scheuerlein, and G. Grasso, "Characterization of mechanical properties of MgB_2 conductor for the superconducting link project at CERN," *IEEE Trans. Appl. Supercond.*, vol. 25, no. 3, Jun. 2015, Art. no. 4801004.

[14] S. Tu, X. Ren, J. He, and Z. Zhang, "Stress-strain curves of metallic materials and post-necking strain hardening characterization: A review," *Fatigue Fract. Eng. Mater. Struct.*, vol. 43, 2020, pp.3–19.

[15] R.M. Digilov, "Flexural vibration test of a cantilever beam with a force sensor: fast determination of Young's modulus," *Eur. J. Phys.*, vol. 29, Apr. 2008, pp.589–597.

[16] *Metals Handbook*, 9th ed., The ASM Handbook Committee, Am. Soc. Metals, Metals Park, OH, USA, 1979, pp.779.

[17] A.S. Tsapleva, I.M. Abdyukhanov, K.O. Bazaleeva, A.A. Aleksandrova, and M.V. Alekseev, "Texture of Nb filaments and Nb_3Sn phase in technical superconductors fabricated by bronze and internal-tin-source techniques," *Phys. Met. Metallogr.*, vol. 121, 2020, pp.471–475.

[18] T.R. Bieler *et al*, "Physical and mechanical metallurgy of high purity Nb for accelerator cavities," *Physical Review Special Topics – Accelerators and Beams*, vol. 13, Mar. 2010, Art. no. 031002.